Polymorphic Behavior of Syndiotactic Poly(*p*-chlorostyrene) and Styrene/*p*-Chlorostyrene Cosyndiotactic Random Copolymers

Anna De Girolamo Del Mauro, Fausta Loffredo, Vincenzo Venditto, Pasquale Longo, and Gaetano Guerra*

Dipartimento di Chimica, Università di Salerno, Via S. Allende, 84081 Baronissi, Salerno, Italy

Received May 22, 2003; Revised Manuscript Received July 28, 2003

ABSTRACT: Cosyndiotactic random copolymers of styrene/*p*-chlorostyrene (S/*p*-CS) have been prepared for the entire composition range. Their polymorphic behavior has been studied by means of wide-angle X-ray diffraction, differential scanning calorimetry, Fourier transform infrared spectroscopy, and ultraviolet spectroscopy. For all samples, the possible formation of clathrate structures has been investigated. A new clathrate phase, being colored and comprising trans planar chains, has been obtained for copolymers with high chlorinated comonomer unit content in the presence of the *p*-chlorostyrene guest. Both colored and trans-planar clathrates are unprecedented for styrene-based syndiotactic homopolymers and copolymers. A phase diagram of this copolymer system in the presence of the *p*-chlorostyrene guest has been reported.

Introduction

The syndiospecific homopolymerization[1−5] and copolymerization[4−7] of styrene and *p*-chlorostyrene (*p*-CS) have been reported in recent years. Structural studies have shown complex polymorphic behaviors for *s*-PS[8−19] as well as for syndiotactic poly(*p*-methylstyrene) (*s*-PPMS)[20−23] and poly(*p*-*n*-butyl-styrene).[24] In particular for *s*-PS, four crystalline forms have been described. The α and β crystalline forms contain molecular chains with a planar zigzag conformation, and the γ and δ crystalline forms contain *s*(2/1)2 helical chains. Variations of the polymorphic behavior of *s*-PS have been observed by introducing different comonomer units (e.g., *p*-methylstyrene,[20−23] *p*-*n*-butylstyrene [24]) into the *s*-PS chain. Particular crystalline forms can be favored by specific combinations of thermodynamic and kinetic effects.[20−25]

Clathrate phases, including several different guest molecules, have been observed and characterized for *s*-PS[8−10,26−30] and *s*-PPMS[31−36] as well as for syndiotactic copolymers based on them.[22,23] All of the presently known clathrate phases from syndiotactic homopolymers and copolymers based on styrene and substituted styrenes contain *s*(2/1)2 helical chains.

Recent studies have shown that the removal of guest molecules from *s*-PS clathrate phases, under suitable conditions,[37−39] produces the nanoporous crystalline δ form, which includes two identical cavities per unit cell, whose shape and volume have been accurately evaluated.[19,40,41] On the basis of this nanoporous phase, thermoplastic molecular sieves, which are promising for applications in chemical separations as well as in water and air purification, have been obtained.[38,40,42] Possible nanoporous crystalline phases of syndiotactic polymers based on substituted styrenes could be helpful in tuning the volume of the cavities and hence the selectivity of these materials. An accurate characterization of clathrate phases for syndiotactic polymers based on substituted styrenes is, of course, preliminary to the possible achievement of corresponding nanoporous phases.

In the present paper, the polymorphic behavior of syndiotactic poly(*p*-chlorostyrene) (*s*-PPCS) as well as of the cosyndiotactic copolymers styrene/*p*-chlorostyrene has been studied. For all samples, the possible formation of clathrate structures has also been investigated, and clathrate structures with the *p*-CS guest have been obtained over the complete range of composition. For the copolymers presenting a content of chlorinated units higher than 39 mol %, a new clathrate phase, which is colored and contains trans planar chains, has been achieved. Both features are unprecedented for syndiotactic homopolymers and copolymers based on styrene and substitutes styrenes.

* Corresponding author. E-mail: gguerra@unisa.it.

Experimental Section

Materials. Styrene and *p*-chlorostyrene were purchased from Aldrich Chemie, kept in contact over calcium hydride for 3 h, and distilled under reduced pressure before use. Toluene was dried by refluxing over Na-benzophenone and distilled before use in a nitrogen atmosphere. Cp^*TiCl_3 (Cp^* = pentamethylcyclopentadienyl), purchased from Aldrich Chemie, was used as received. Methylalumoxane (MAO) was provided by Witco Gmbh as a 10 wt % solution in toluene and used as a solid after the distillation of solvent.

Polymerizations. Polymerizations were performed for 1 h at 50 °C or for 6 h at 20 °C in a stirred 250-mL flask under a nitrogen atmosphere using toluene (30 mL) as a solvent and a Cp^*TiCl_3 (6×10^{-6} mol) catalyst activated with MAO (6×10^{-3} mol based on Al).

All copolymerizations were stopped by pouring the reaction mixture into a large amount of acidified methanol. The polymers were recovered by filtration, washed with fresh methanol, and dried under vacuum.

The insoluble polymer fraction as determined by a conventional extraction procedure (for 3 h with boiling 2-butanone in a Kumagawa extractor) was for all samples larger than 90 wt %. Except for the *s*-PPCS homopolymer, all samples were fully soluble in hot chloroform. *s*-PPCS was completely soluble in hot *p*-chlorostyrene.

Polymer Characterization. ^{13}C NMR spectra were measured with an AM250 Bruker spectrometer at 120 °C in a solution of tetrachlorodideuteroethane. Copolymer compositions were evaluated from the ratio of the areas of the signals of the quaternary carbons. The concentrations of the stereochemical tetrads were determined from the areas of the methylene resonances.[4] The fraction of *rrr* tetrads was for all samples higher than 95%.

The clathrate samples with *p*-CS were obtained by immersing the powder samples into the liquid solvent for 1 h or by

10.1021/ma034678l CCC: $25.00
Published on Web 09/11/2003

casting procedures using 3 wt % solutions. As-polymerized and clathrate samples were held in air at room temperature for at least 12 h before analyses.

Wide-angle X-ray diffraction (WAXS) patterns were obtained with an automatic 1710 Philips powder diffractometer using nickel-filtered Cu Kα radiation. A crystallinity index has been determined by resolving the diffraction pattern in a selected 2θ range (5−38°) into two areas A_c and A_a that can be taken as being proportional to the crystalline and amorphous weight fractions, respectively, and calculated through the expression $100A_c/(A_c + A_a)$. Quenched samples were used to obtain X-ray diffraction patterns of completely amorphous samples.

The content of volatile organic molecules in clathrate samples was evaluated by thermogravimetric analysis carried out with a Mettler TG50 thermobalance in a flowing nitrogen atmosphere at a heating rate of 10 °C/min.

UV−visible spectra were obtained with a Perkin-Elmer LAMBDA EZ-201 spectrophotometer. Polymer films of thickness close to 10 μm and the solutions were contained in 0.1- and 1.0-cm path-length cells, respectively.

Fourier transform infrared (FTIR) spectra were obtained with a Brucker Vector 22 spectrophotometer. The scanned wavenumber range was 400−4000 cm^{-1} at resolution of 1 cm^{-1}. Typically, 32 spectra were signal-averaged in the conventional manner to reduce spectral noise. The reported results were obtained by using film samples or polymer solutions.

Differential scanning calorimetry (DSC) measurements were carried out with a DSC 2920 TA instrument in a nitrogen flow by using a heating and cooling rate of 10 °C/min. The peak temperatures of the melting endotherms and of the crystallization exotherms have been indicated as melting temperature and crystallization temperature, respectively.

Results and Discussion

X-ray Diffraction Analysis. As-Polymerized Samples. The X-ray diffraction patterns of as-polymerized homopolymers and copolymers are shown in Figure 1.

The patterns of copolymers with chlorinated unit content lower than 29 mol % (Figure 1b and c) are characterized by peaks at $2\theta_{(Cu\ K\alpha)} \cong 7.9$, 10.2, 17.3, 20.0, and 23.1°, which are slightly shifted at lower diffraction angles with respect to the *s*-PS/styrene clathrate sample (Figure 1a) characterized by peaks at $2\theta_{(CuK\alpha)} \cong 8.0$, 10.3, 17.4, 20.2, and 23.4° corresponding to 010, $\bar{2}10$, 111, $\bar{3}21-301$, and $\bar{4}11$ reflections, respectively, of the typical monoclinic cell of *s*-PS clathrates.[26−30] Similar behaviors have also been observed for cosyndiotactic copolymers of styrene with low contents of *p*-methylstyrene[20,23] and *p*-*n*-butylstyrene[24] comonomer units.

The pattern of the *s*-PPCS homopolymer presents several crystalline reflections at $2\theta \cong 9.7$(w), 11.2(s), 12.0(w), 14.8(m), 19.4(s), 20.8(s), 22.2(w), 27.0(w), 28.5-(w), 29.5(w), 31.5(w), 35.0(w), and 39.0°(w) (w = weak, m = medium, s = strong; see Figure 1f). The crystallinity index, obtained as described in the Experimental Section, has been evaluated close to 50%.

For as-polymerized copolymers with high chlorinated unit content, the X-ray diffraction patterns (Figure 1d and e) present amorphous halos together with very weak reflections at $2\theta \cong 8.5$, 9.7, and 14°.

Annealed Samples. The X-ray diffraction patterns of the as-polymerized samples of Figure 1a−f after thermal annealing at 170°C are reported in Figure 2a−f, respectively.

As usual for this kind of thermal treatment,[10,11,23] the clathrate phase of *s*-PS (Figure 1a) is transformed into the crystalline helical γ phase (Figure 2a). For copolymers with chlorinated unit content equal to or lower than 29 mol %, the clathrate phase (Figure 1b and c) is transformed into a crystalline α phase

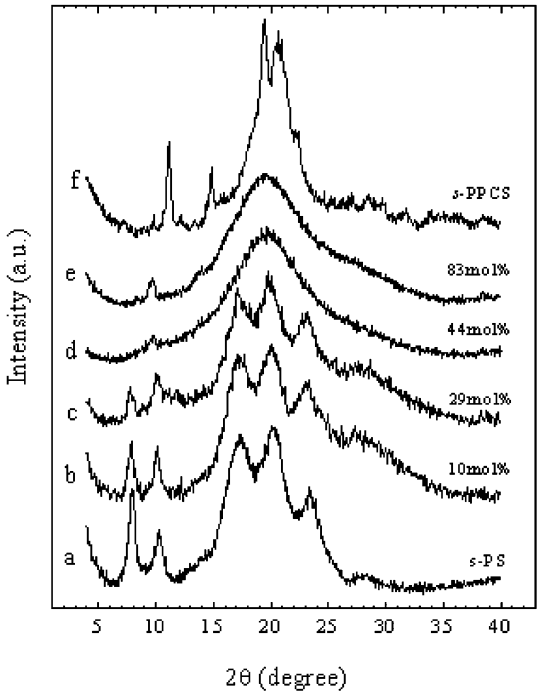

Figure 1. X-ray diffraction patterns (Cu Kα) of as-polymerized samples. For copolymer samples, the molar content of chlorinated units is indicated.

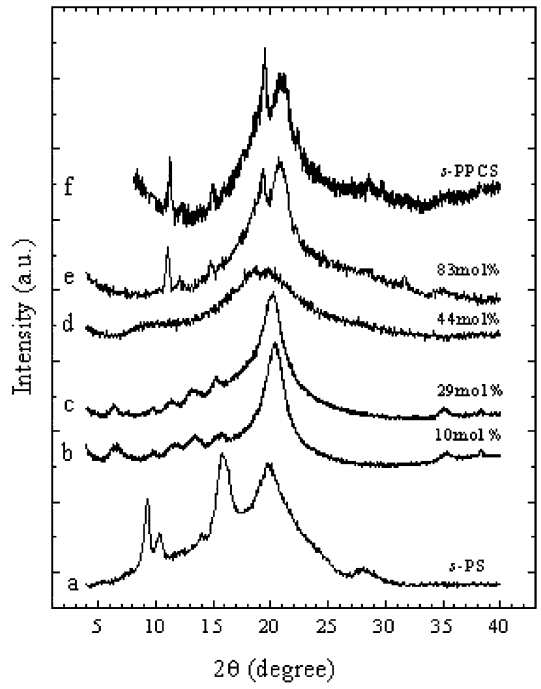

Figure 2. X-ray diffraction patterns (Cu Kα) of the samples in Figure 1 after annealing at 170 °C. For copolymer samples, the molar content of chlorinated units is indicated.

(Figure 2b and c), which for *s*-PS is generally obtained for thermal treatments above 180 °C.[8,10,11] It is worth noting that for our copolymers, whose chlorinated monomer unit content is at least 10 mol %, all attempts to achieve the γ form by thermal annealing procedures at different temperatures were unsuccessful.

The pattern for the *s*-PPCS sample (Figure 2f) remains essentially unaltered as a consequence of the thermal treatment, except for the disappearance of the weak peak at 9.7° (Figure 1f).

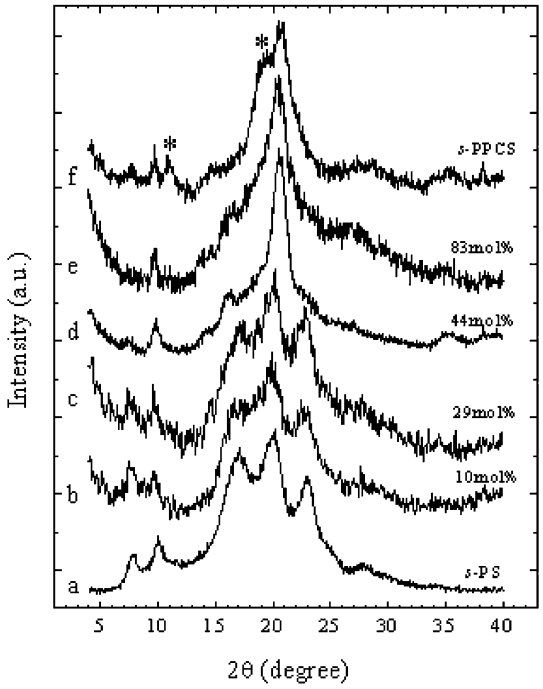

Figure 3. X-ray diffraction patterns (Cu Kα) of samples treated with *p*-CS. For copolymer samples, the molar content of chlorinated units is indicated. Peaks of the usual crystalline phase of *s*-PPCS (Figures 1f and 2f) are indicated by stars on curve f.

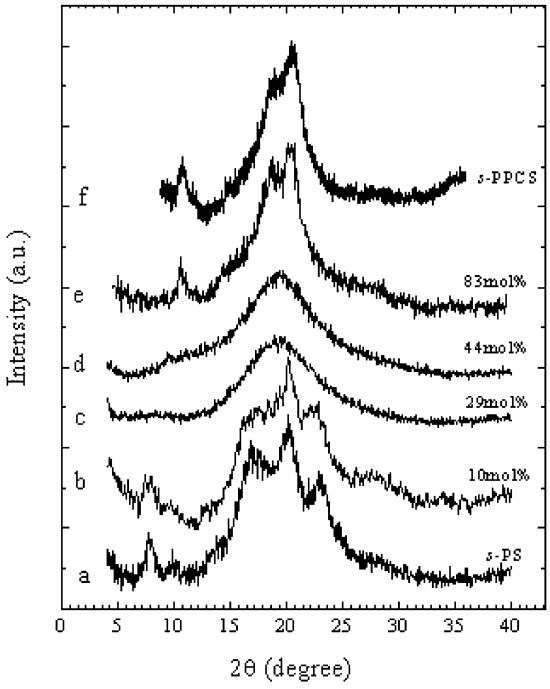

Figure 4. X-ray diffraction patterns (Cu Kα) of the *p*-CS-treated samples of Figure 3 after *p*-CS removal by extraction with boiling acetone. For copolymer samples, the molar content of chlorinated units is indicated.

As for the copolymers with high chlorinated unit content, the very weak peaks, which are present in the as-polymerized samples (Figure 1d and e), disappear as a consequence of the annealing. In particular, the copolymer with 39 and 44 mol % (Figure 2d) chlorinated units becomes fully amorphous, and the copolymer with 83 mol % chlorinated units (Figure 2e) crystallizes in a form similar to that of *s*-PPCS (Figure 2f).

Samples Treated with *p*-CS. As-polymerized samples of Figure 1, after room-temperature treatments with *p*-CS, present the X-ray diffraction patterns shown in Figure 3. In particular, as for *s*-PS and copolymer samples, 1 h of treatment is sufficient to produce the changes from the X-ray diffraction patterns of Figure 1a−e to those of Figure 3a−e, but for *s*-PPCS, the change from the X-ray diffraction pattern of Figure 1f to that of Figure 3f is achieved after 1 month of treatment. First, it is worth noting that as a consequence of this procedure not only both homopolymers but also all copolymers, over the entire composition range, have a high crystallinity content. The residual solvent content, as evaluated by thermogravimetric analysis, is in the range 20−30 wt % for all samples, but for *s*-PPCS, it is close to 10%.

The X-ray diffraction of the *s*-PS sample (Figure 3a) is clearly that of an *s*-PS/ *p*-CS clathrate. In fact, it is similar to those of other *s*-PS clathrates and, in particular, to that of the *s*-PS/styrene clathrate (Figure 1a). The most relevant differences refer to the two peaks in the low 2θ region (corresponding to the 010 and $\bar{2}10$ reflections), which for the clathrate with styrene (Figure 1a) and with *p*-CS (Figure 3a) are located at 8.0, 10.3° and at 7.9, 10.1°, respectively. Moreover, the ($\bar{2}10$) reflection is more intense than the (010) reflection, as already observed for other *s*-PS clathrates containing halogenated guests.[10,38]

The X-ray diffraction patterns of copolymer samples with chlorinated unit content up to 29 mol % (Figure 3b and c) are similar to those obtained for *s*-PS (Figure 3a) and clearly indicate the presence of clathrate phases similar to that obtained for *s*-PS.

Copolymers with higher chlorinated unit content (39, 44, and 83 mol %) are readily dissolved by *p*-CS, hence the solvent treatment results in solution cast films. These films are yellow (as shown in the UV−vis spectra described in the next section), and their X-ray diffraction patterns (Figure 3d and e) show the occurrence of a new crystalline phase that presents reflections at $2\theta_{(\text{Cu K}\alpha)} \cong$ 7.5(w), 9.7(s), 14.2(w), 16.3(m), 20.5(vs), and 35.0°-(m).

Some of these reflections at $2\theta \cong 7.5$, 9.7, and 35.0° are also clearly present in the X-ray diffraction pattern of *s*-PPCS (Figure 3f), together with the main reflections of the annealed sample (Figure 2f) at $2\theta \cong 11.2$ and 19.4° (indicated by a star in Figure 3f). Moreover, the most intense reflection of Figure 3f is located at $2\theta \cong$ 20.7 °C, that is, intermediate between the most intense reflections of the patterns of Figure 3d (20.5°) and of Figure 2f (20.8°).

Analogous casting procedures from several different solvents (including benzene, chlorobenzene, fluorobenzene, 1,2-dichlorobenzene, *o*-chlorophenol, and *p*-methylstyrene) do not induce crystallization to copolymer samples with high chlorinated unit content (39, 44, and 83 mol %).

Samples Treated with *p*-CS after *p*-CS Extraction. The X-ray diffraction patterns of the *p*-CS-treated samples of Figure 3, after *p*-CS removal by extraction with boiling acetone, are shown in Figure 4. The residual solvent content, as evaluated by thermogravimetric analyses, is lower than 1−2 wt % for all films.

The X-ray diffraction of the *s*-PS sample (Figure 4a) is that of a nanoporous δ phase,[19] as generally occurs

for these kinds of treatments on *s*-PS clathrate - phases.[37−39]

The X-ray diffraction patterns of copolymer samples with chlorinated unit content up to 10 mol % (Figure 4b) also show the presence of the nanoporous δ phase, and those of copolymer samples with chlorinated unit content in the range of 17−44 mol % (Figure 4c and d) show only amorphous halos. The X-ray diffraction patterns of the copolymer sample with the highest chlorinated unit content (83 mol %, Figure 4e) and of the *s*-PPCS homopolymer (Figure 4f) show only the crystalline reflections that are present in the annealed samples (Figure 2e and f), and all reflections that characterize the crystalline phase induced by *p*-CS treatment (Figure 3d and e, also present as minor peaks in Figure 3f) are completely absent.

In summary, the X-ray diffraction patterns of Figures 1−4 show that *s*-PPCS and copolymers with high chlorinated unit content present two crystalline phases: the first is obtained by melt crystallization or by annealing, and the second one is *p*-CS-induced. Only the *p*-CS-induced crystalline phase has been observed for the copolymer samples with 39 and 44 mol % chlorinated units.

Several attempts to get oriented samples from *s*-PPCS and copolymers with chlorinated unit content equal to or higher than 39 mol % were unsuccessful, possibly because of the low molecular masses associated with the low reactivity of the chlorinated comonomer. Hence, information relative to the polymer conformation into these two crystalline phases was not directly available from X-ray diffraction data. However, for the *p*-CS-induced crystalline phase, the presence of a well-defined diffraction peak at 2θ (Cu Kα) $\approx$ 35° (Figure 3d), corresponding to a Bragg distance $d \approx 5.1$ Å, suggests the possible presence of trans planar polymer chains. It is worth noting that an analogous diffraction peak is present for all crystalline phases based on *s*-PS, which include trans planar chains such as the α-phase samples shown in Figure 2b,c.

The presence of a substantial amount of *p*-CS in the films of Figure 3 and the occurrence of crystallization, for random copolymers with nearly equimolar amounts of comonomer units, suggest that the *p*-CS-induced crystalline phase could be a clathrate phase, as already observed for the THF-induced crystalline phase of the analogous S/*p*-MS cosyndiotactic copolymers.[23]

UV−Visible Spectroscopy. *s*-PPCS and the copolymer samples, which present the new *p*-CS-induced crystalline phase (Figure 3d−f), show an intense yellow color, but *s*-PS and copolymer samples with lower chlorinated unit content (Figure 3a−c) are not colored.

This yellow color disappears when the *p*-CS-induced crystalline phase is removed. In particular, after *p*-CS extraction, both the copolymer films with 83 mol % chlorinated units (Figure 3e), which present a crystalline phase transition (Figure 4e), as well as the copolymer films with 44 mol % chlorinated units (Figure 3d), which become amorphous (Figure 4d), lose their yellow color.

This is shown, for instance, by the UV−vis absorption spectra of films of the copolymers with 44 and 83 mol % chlorinated units cast from *p*-CS (curves a) after *p*-CS extraction (curves b) or cast from chloroform (curves c); these are shown in Figure 5 for the spectral range of 300−600 nm.

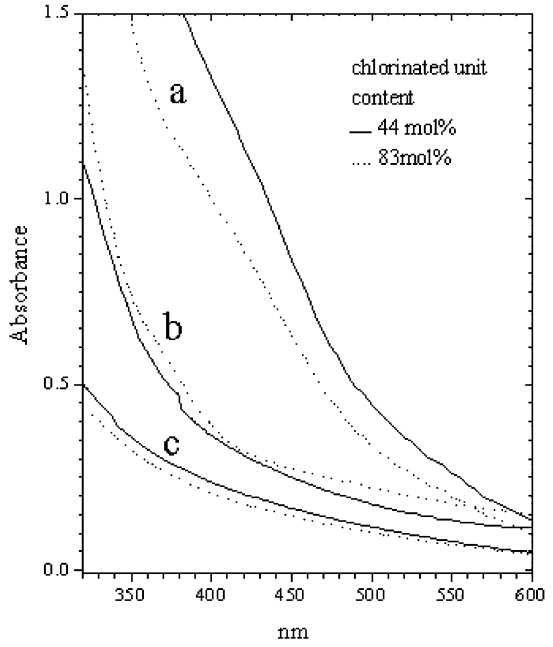

Figure 5. UV−vis absorption spectra in the 300−600 nm range for copolymer films with 83 mol % (· · ·) and 44 mol % (—) chlorinated monomeric units: (a) cast from *p*-CS (b) cast from *p*-CS after *p*-CS extraction, and (c) cast from $CHCl_3$.

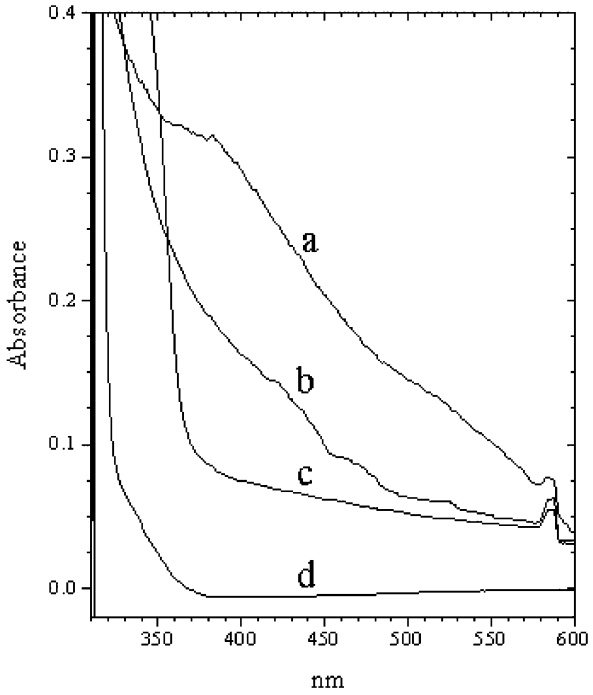

Figure 6. UV−vis absorption spectra in the 300−600 nm range of 1 wt % polymer solutions in *p*-CS 1 h after preparation: (a) *s*-PPCS, (b) copolymer with 83 mol % chlorinated units, and (c) *s*-PS. The absorption spectrum of liquid *p*-CS is shown by curve d.

It is worth noting that, for *s*-PPCS and copolymer samples with chlorinated unit content higher than or equal to 39 mol %, *p*-CS solutions are not colored as soon as they are prepared but become gradually yellow with time. For instance, the UV−vis absorption spectra of Figure 6 shows the absorption spectra of 1 wt % polymer solutions obtained 1 h after preparation. It is clearly apparent that the *p*-CS solutions of *s*-PPCS (Figure 6a) and of the copolymer with 83 mol % chlorinated units (Figure 6b) exhibit an intense absorption, gradually

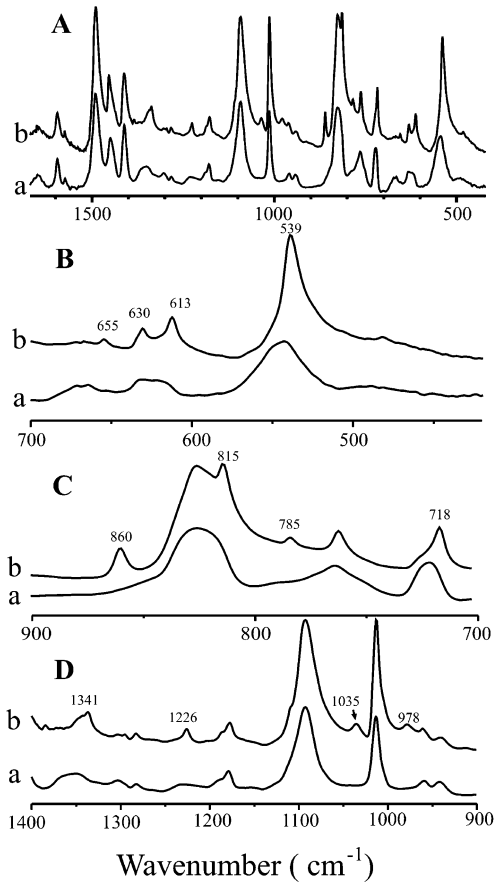

Figure 7. (a) IR spectra of atactic PPCS and of (b) as-polymerized crystalline syndiotactic PPCS in the (A) 400−1700, (B) 400−700, (C) 700−900, and (D) 900−1400 cm^{-1} spectral regions. The wavenumbers corresponding to the main crystalline peaks are indicated close to curves b.

decreasing in the spectral range of 300−600 nm. In contrast, the *p*-CS solution of *s*-PS has essentially no absorption in the visible spectral range (Figure 6c), as also occurs for liquid *p*-CS (Figure 6d).

It is also worth adding that all solutions and cast films of our homopolymer and copolymer samples when prepared from all of the examined solvents different from *p*-CS are not colored. Moreover, *p*-CS solutions and films cast from *p*-CS solutions of the corresponding atactic homopolymer (a-PPCS) are also not colored.

In summary, the UV−vis data of this section suggests that the observed absorption in the visible spectral range is associated with specific interactions between the syndiotactic *p*-CS-based polymers and the *p*-CS solvent. Because this kind of visible-light absorption has been observed for our solid samples only when the *p*-CS-induced crystalline phase is present, the latter is expected to involve polymer−solvent interactions analogous to those observed for *p*-CS solutions. This would be compatible with the nature of clathrate phase for the *p*-CS-induced crystalline phase, as already suggested by gravimetric and X-ray diffraction data of the previous section.

Fourier Transform Infrared Analysis. The FTIR spectra of an amorphous atactic PPCS film and of a KBr pellet including a semicrystalline powder of *s*-PPCS, presenting X-ray diffraction patterns such as that in Figure 1f, are compared in Figure 7 (curves a and b, respectively). The FTIR spectrum of amorphous *s*-PPCS, obtained by quenching from the melt, is very similar to that of *a*-PPCS, shown by curves a of Figure 7.

The comparison clearly shows the occurrence for *s*-PPCS of several infrared absorbance peaks associated with macromolecules in the crystalline phase: 1341(w), 1226(m), 1035(m), 978(m), 860(s), 815(s), 785(m), 718-(s), 655(w), 630(m), 613(m), and 539(vs) cm^{-1}. Some of these crystalline peaks are very close to those that have been observed for crystalline and mesomorphic phases of *s*-PPMS including trans planar chains: 1334(m), 1222(s), 976(m), 858(s), 718(s), and 540(vs) cm^{-1}.[43] Moreover, for *s*-PS, the spectra of the crystalline forms with trans planar chains (α and β forms) are also characterized by well-defined crystalline bands at 1336 (β form), 1330 (α form), 1222, and 540 cm^{-1}. (See, for example, Figure 6 of ref 11.) Particularly informative is the spectral region of 500−600 cm^{-1}, which generally includes, for styrene-based syndiotactic polymers, only one intense peak located near 540 cm^{-1} for trans planar crystalline phases and additional intense peaks located near 500 and 570 cm^{-1} for helical crystalline phases.[11,43] Hence, the FTIR data (Figure 7B) clearly indicate that the *s*-PPCS crystalline phase includes trans planar chains.

FTIR spectra of three different films obtained by the copolymer sample with 83 mol % chlorinated units are compared in Figure 8. Curves a correspond to an amorphous film obtained by quenching from the melt. Curves b correspond to a quenched film annealed at 170 °C, which presents an X-ray diffraction pattern similar to those of Figure 2e or 4e and hence presents a crystalline phase analogous to that observed for *s*-PPCS. Curves c correspond to a film cast from *p*-CS solution, which presents an X-ray diffraction pattern similar to that of Figure 3e and hence includes the *p*-CS clathrate phase. On the c curves, the most relevant *p*-CS absorption peaks are also explicitly labeled.

The spectral comparison of Figure 8 shows that both crystalline (curves b) and clathrate (curves c) phases present well-defined trans planar bands: 1341, 1227, 1030, 860, 785 (Figure 8C, curve b), 789 (Figure 8C, curve c), and 539 cm^{-1}. This clearly indicates that the crystalline clathrate phase induced by *p*-CS, which according to the previous sections is responsible for the yellow color of the samples, includes trans planar chains.

As for the colored solutions of *s*-PPCS and of copolymers with high chlorinated unit content, particularly informative is the very intense 539-cm^{-1} peak. As an example, the FTIR spectra in the 520−720 cm^{-1} range of a colorless *p*-CS solution of a copolymer with low chlorinated unit content (10 mol %, curve a), of a yellow *p*-CS solution (curve b), and of a colorless *p*-MS solution (curve c) of a copolymer with high chlorinated unit content (83 mol %) are compared in Figure 9.

It is apparent (also by comparison with the absorption spectra of the pure solvents shown as dotted lines close to curves a and c) that only the colored solution in *p*-CS presents a well-defined peak at 539 cm^{-1}, corresponding to long trans planar sequences (Figure 9b).

The results of Figures 8 and 9 suggest that the visible-light absorption producing the yellow color would be associated with polymer/*p*-CS interactions involving polymeric stretches being in the trans conformation, which would occur, for copolymers with high chlorinated unit content, both in the clathrate phases with *p*-CS and in *p*-CS solutions.

Differential Scanning Calorimetry. DSC scans of homopolymers and copolymers, after *p*-CS treatments,

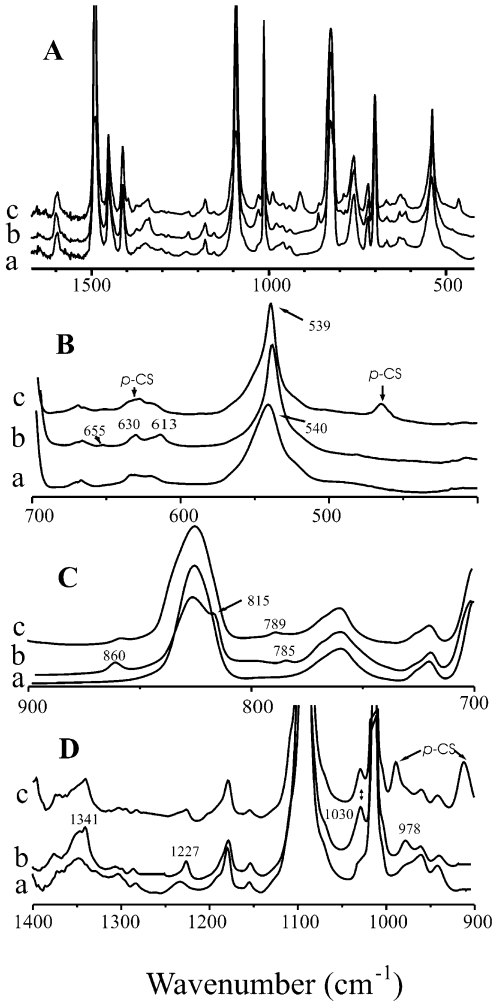

Figure 8. IR spectra in the (A) 400−1700, (B) 400−700, (C) 700−900, and (D) 900−1400 cm^{-1} spectral regions of the copolymer with 83 mol % chlorinated comonomer units: (a) amorphous film, (b) film with thermally induced crystallinity (Figure 2e), and (c) yellow film with *p*-CS-induced crystallinity (Figure 3e, *p*-CS clathrate). The wavenumbers corresponding to the main crystalline peaks are indicated close to curves b and c. The absorption peaks of *p*-CS are explicitly labeled on curves c.

whose X-ray diffraction patterns are shown in Figure 3a−f are reported in Figure 10a−f, respectively. The corresponding second heating scans, after cooling from the melt at a rate of 10 °C/min, are reported in Figure 11a−f, respectively.

The DSC scan of *s*-PS (Figure 10a) is similar to those reported in the literature for other clathrate samples with different guests.[10,18] The variation of specific heat typical of a glass transition is hidden by a broad endothermic peak due to guest release associated with clathrate → γ-phase transition. An intense endothermic peak, centered at 270 °C, corresponds to the melting of α-form crystals.

Copolymer samples with chlorinated units up to 29 mol % present DSC scans similar to that of *s*-PS, but both the temperature and enthalpy of melting decrease progressively with the increase in chlorinated comonomer content (Figure 10b and c). The second heating scans of Figure 11a−c, which are not disturbed by solvent release, besides melting clearly show the glass transition. As for the copolymer sample with 29 mol % chlorinated units, crystallization on heating (Figure 11c) centered nearly at 175 °C is also apparent.

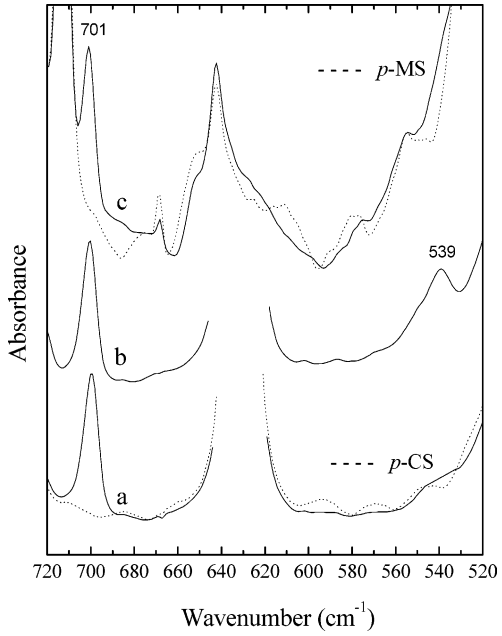

Figure 9. IR spectra in the 520−720 cm^{-1} spectral region of 3 wt % polymer solutions: (a) colorless *p*-CS solution of the copolymer with 10 mol % chlorinated comonomer units, (b) yellow *p*-CS solution of the copolymer with 83 mol % chlorinated comonomer units, and (c) colorless *p*-MS solution of the copolymer with 83 mol % chlorinated comonomer units. Absorption spectra of pure *p*-CS and *p*-MS solvents are shown as dotted lines close to curves a and c.

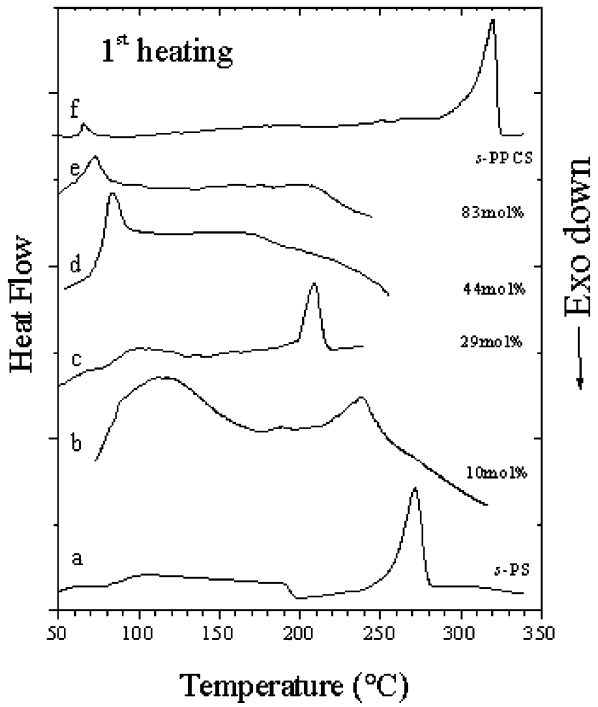

Figure 10. DSC scans corresponding to the first heating of samples treated with *p*-CS, whose X-ray diffraction patterns are shown in Figure 3a−f. For copolymer samples, the molar content of chlorinated comonomer units is indicated.

The melt-crystallized *s*-PPCS sample (second heating DSC scan of Figure 11f) shows together with a glass transition at 127 °C a melting endothermic peak, centered at 324° C with a melting enthalpy close to 23 J/g.

The DSC scans of copolymer samples with chlorinated unit content higher than 39 mol % when cast from *p*-CS

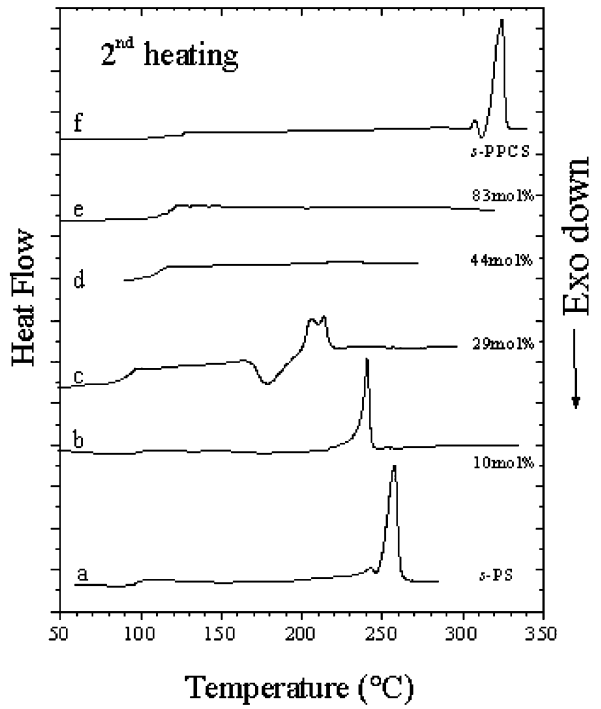

Figure 11. DSC scans corresponding to the second heating, after cooling from the melt at a rate of 10 °C/min, for the samples of Figure 10.

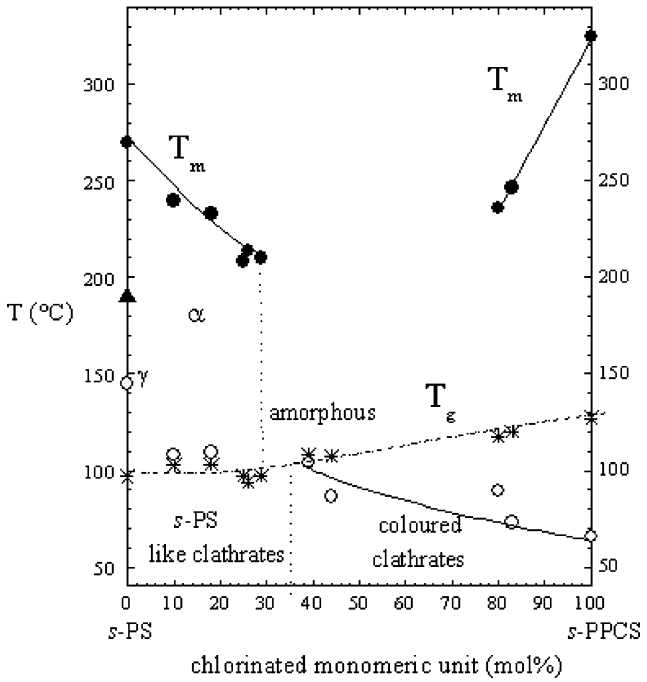

Figure 12. Phase diagram of copolymer system S/*p*-CS, which includes crystalline and *p*-CS clathrate phases. It has been constructed by reporting the melting temperatures (●) and temperatures of guest loss from clathrate phases (○) observed in DSC scans of samples treated with *p*-CS (such as those of Figure 10) as a function of *p*-CS content. The glass-transition temperatures, obtained by second heating DSC scans (such as those of Figure 11), are indicated by stars (*) and are fitted by a dashed line.

solution show only a small endothermic peak (the maximum enthalpy change being close to 5 J/g of desiccated polymer) located in the temperature range of 60−90 °C (Figure 10d and e). These endothermic peaks correspond to the melting of the *p*-CS-induced crystalline phase, whose X-ray diffraction pattern is shown in Figure 3d and e. A small endothermic peak located nearly at 60 °C is present also for the *s*-PPCS homopolymer (Figure 10f) and corresponds to the melting of a minor polymer fraction, which presents the *p*-CS-induced crystalline phase (Figure 3f). These copolymer samples with *p*-CS content higher than 39 mol % do not crystallizes on cooling from the melt, hence the second heating runs show only glass-transition temperatures (Figure 11d and e).

Copolymer System Phase Diagram Including *p*-CS Clathrate Phases. The results presented in the previous sections show that clathrate phases including *p*-CS are formed over the entire copolymer composition range and that these clathrate phase are transformed by thermal treatments, which remove the guest *p*-CS molecules, into crystalline or amorphous phases.

The first heating DSC scans (such as those of Figure 10) can include high-temperature endothermic peaks (T > 200 °C) corresponding to the melting of crystalline phases and/or low-temperature endothermic peaks (T < 100 °C) corresponding to guest loss from clathrate phases. This guest loss generally leads to a complete loss of crystalline order, but for the copolymers with chlorinated unit content lower than 30 mol %, the guest loss leads to *s*-PS α-phase formation. This interpretation of the DSC endothermic peaks has been confirmed by X-ray diffraction patterns of samples annealed at different temperatures.

The melting temperatures of crystalline phases of copolymers with high chlorinated unit content have been taken by DSC scans of samples annealed at 170 °C, which present X-ray diffraction patterns such as that of Figure 2e. All of these temperatures of melting of crystalline phases and of guest loss from clathrate phases as well as the glass-transition temperatures, taken from second heating scans (such as those of Figure 11), are reported as function of the chlorinated monomer unit content in Figure 12.

The *s*-PS-like clathrate → α transition remains close to the glass transition temperature, and the melting temperatures of the α form markedly decrease with increasing chlorinated comonomer unit content. These data indicate that the introduction of *p*-CS comonomer units into *s*-PS chains gradually reduces the stability of the trans planar α form but more strongly destabilizes the helical γ form.

For copolymers with 39 and 44 mol % chlorinated units, the only observed crystalline phase is a clathrate with *p*-CS, and a direct transition from the clathrate phase to the amorphous phase is observed.

For copolymers with chlorinated unit content higher than 79 mol %, the semicrystalline samples including the clathrate phase with *p*-CS are transformed into amorphous samples for intermediate annealing temperatures. For high annealing temperatures, crystallization into a high-melting crystalline form similar to that observed for *s*-PPCS is achieved.

Conclusions

Syndiotactic poly(*p*-chlorostyrene) and cosyndiotactic copolymers of styrene with *p*-CS of different compositions have been obtained by using the Cp*$TiCl_3$ with MAO catalytic system.

s-PPCS is crystalline as polymerized and easily crystallizes from the melt. The melting point (T_m = 324

°C) is significantly higher than for *s*-PS (T_m = 260 °C). FTIR measurements clearly show that, as usual for syndiotactic polymers based on styrene and substituted styrenes,[10,29] this high-melting crystalline phase includes trans planar chains.

Copolymers with chlorinated unit content lower than 30 mol % easily crystallize into the α phase of *s*-PS, and the γ phase has not been obtained, at least for chlorinated unit content higher than 10 mol %.

Copolymers with chlorinated unit content higher than 79 mol % can crystallize by thermal annealing into a crystalline form similar to that observed for *s*-PPCS.

Clathrate structures with *p*-CS molecules have been observed over the whole range of composition. In particular for copolymers with chlorinated unit content equal to or lower than 30 mol %, crystalline clathrate forms, which contain s(2/1)2 helices and a packing similar to that of the δ phase of *s*-PS, have been obtained. For copolymers with chlorinated unit content equal to or higher than 39 mol %, a new colored clathrate phase is obtained. This new clathrate phase is yellow and includes trans planar chains.

The absorption of visible light as a consequence of intermolecular host−guest interactions in clathrate structures has already been observed, for instance, for sulfur dioxide-β quinol clathrates.[44] To our knowledge, it has never been observed for clathrates with polymeric hosts. Moreover, a clathrate phase including trans planar chains is unprecedented for syndiotactic polymers based on styrene and substituted styrenes.

Trans planar chains and visible-light absorption (leading to a yellow color) have been also observed for *p*-CS solutions of *s*-PPCS and of copolymers with chlorinated unit content higher than 39 mol % but are not present for solutions of the same polymers in other solvents or for *p*-CS solutions of other styrene and substituted styrene homopolymers and copolymers. This suggests that similar interactions between *p*-CS molecules and trans planar polymer stretches, including *p*-CS comonomer units, would be present in both *p*-CS solutions and *p*-CS clathrate phases.

Further studies are needed to establish the structure of this new trans planar clathrate phase as well as to obtain more detailed information relative to the supramolecular interactions giving rise to light absorption in the visible region.

A phase diagram of the copolymer system, which includes crystalline and *p*-CS clathrate phases, has been constructed on the basis of glass-transition, melting, and solid−solid transition temperatures observed by DSC scans.

Acknowledgment. The financial support of MURST of Italy (Grants PRIN 2002 and Cluster 26) and Regione Campania (Legge 41 and Centro di Competenza Regionale CdCR Nuove Tecnologie per le Attivita' Produttive) is acknowledged.

References and Notes

(1) Ishihara, N.; Seimiya, T.; Kuramoto, M.; Uoi, M. *Macromolecules* **1986**, *19*, 2465.
(2) (a) Zambelli, A.; Longo, P.; Pellecchia, C.; Grassi, A. *Macromolecules* **1987**, *20*, 2035. (b) Pellecchia, C.; Longo, P.; Grassi, A.; Ammendola, P.; Zambelli, A. *Makromol. Chem., Rapid Commun.* **1987**, *8*, 277.
(3) (a) Ishihara, N.; Kuramoto, M.; Uoi, M. *Macromolecules* **1988**, *21*, 3356. (b) Tomotsu, N.; Ishihara, N.; Newman, T. H.; Malaga, M. T. *J. Mol. Catal. A: Chem.* **1998**, *128*, 167.
(4) Longo, P.; Proto, A.; Zambelli, A. *Macromol. Chem. Phys.* **1995**, *196*, 3015.
(5) Soga, K.; Nakatani, H.; Monoi, T. *Macromolecules* **1990**, *23*, 953.
(6) Grassi, A.; Longo, P.; Proto, A.; Zambelli, A. *Macromolecules* **1989**, *22*, 104.
(7) Zambelli, A.; Pellecchia, C.; Oliva, L.; Longo, P.; Grassi, A. *Makromol. Chem.* **1991**, *192*, 223.
(8) Immirzi, A.; de Candia, F.; Iannelli, P.; Vittoria, V.; Zambelli, A.; *Makromol. Chem., Rapid Commun.* **1988**, *9*, 761.
(9) Greis, O.; Xu, Y.; Asano, T.; Petermann, J. *Polymer* **1989**, *30*, 590.
(10) Guerra, G.; Vitagliano, V. M.; De Rosa, C.; Petraccone, V.; Corradini, P. *Macromolecules* **1990**, *23*, 1539.
(11) Guerra, G.; Musto, P.; Karasz, F. E.; Mackinight, W. J. *Makromol. Chem.* **1990**, *191*, 2111.
(12) De Rosa, C.; Guerra, G.; Petraccone, V.; Corradini, P. *Polym. J.* **1991**, *23*, 1435.
(13) Guerra, G.; De Rosa, C.; Vitagliano, V. M.; Petraccone, V.; Corradini, P. *J. Polym. Sci., Polym. Phys. Ed.* **1991**, *29*, 265.
(14) Guerra, G.; De Rosa, C.; Vitagliano, V. M.; Petraccone, V.; Corradini, P.; Karasz, F. E. *Polym. Commun.* **1991**, *32*, 30.
(15) Rapacciuolo, M.; De Rosa, C.; Guerra, G.; Mensitieri, G.; Apicella, A.; Del Nobile, M. A. *J. Mater. Sci. Lett.* **1991**, *10*, 1084.
(16) Chatani, Y.; Shimane, Y.; Inoue, Y.; Inagaki, T.; Ishioka, T.; Ijitsu, T.; Yukinari, T. *Polymer* **1992**, *33*, 488.
(17) De Rosa, C.; Rapacciuolo, M.; Guerra, G.; Petraccone, V.; Corradini, P. *Polymer* **1992**, *33*, 1423.
(18) Petraccone, V.; Auriemma, F.; Dal Polggetto, F.; De Rosa, C.; Guerra, G.; Corradini, P. *Makromol. Chem.* **1993**, *194*, 1335.
(19) De Rosa, C.; Guerra, G.; Petraccone, V.; Pirozzi, B. *Macromolecules* **1997**, *30*, 4147.
(20) Manfredi, C.; Guerra, G.; De Rosa, C.; Busico, V.; Corradini, P. *Macromolecules* **1995**, *28*, 6508.
(21) Nakatani, H.; Nitta, K.; Soga, K.; Takata, T. *Polymer* **1997**, *38*, 4751.
(22) Loffredo, F.; Pranzo, A.; Guerra, G.; Venditto, V.; Longo, P. *Macromol. Symp.* **2001**, *166*, 165.
(23) Loffredo, F.; Pranzo, A.; Venditto, V.; Longo, P.; Guerra, G. *Macromol. Chem. Phys.* **2003**, *204*, 859.
(24) Thomann, R.; Sernetz, F.; Heinemann, J.; Steinmann, S.; Mülhaupt, R.; Kressler, J. *Macromolecules* **1997**, *30*, 8401.
(25) Corradini, P.; Guerra, G. *Adv. Polym. Sci.* **1992**, *100*, 183.
(26) Chatani, Y.; Shimane, Y.; Inagaki, T.; Ijitsu, T.; Yukinari, T.; Shikuma, H. *Polymer* **1993**, *34*, 1620.
(27) Chatani, Y.; Inagaki, T.; Shimane, Y.; Shikuma, H. *Polymer* **1993**, *34*, 4841.
(28) De Rosa, C.; Rizzo, P.; Ruiz de Ballesteros, O.; Petraccone, V.; Guerra, G. *Polymer* **1999**, *40*, 2103.
(29) Moyses, S.; Sonntag, P.; Spells, S. J.; Laveix, O. *Polymer* **1998**, *39*, 3665.
(30) Yoshioka A.; Tashiro, K. *Macromolecules* **2003**, *36*, 3593.
(31) Iuliano, M.; Guerra, G.; Petraccone, V.; Corradini, P.; Pellecchia, C. *New Polym. Mater.* **1992**, *3*, 133.
(32) Dell'Isola, A.; Floridi, G.; Rizzo, P.; Ruiz de Ballesteros, O.; Petraccone, V. *Macromol. Symp.* **1997**, *114*, 243.
(33) Petraccone, V.; La Camera, D.; Pirozzi, B.; Rizzo, P.; De Rosa, C.; *Macromolecules* **1998**, *31*, 5830.
(34) Petraccone, V.; La Camera, D.; Caporaso, L.; De Rosa, C.; *Macromolecules* **2000**, *33*, 2610.
(35) La Camera, D.; Petraccone, V.; Artimagnella, S.; Ruiz de Ballesteros, O. *Macromolecules* **2001**, *34*, 7762.
(36) Petraccone, V.; Tarallo, O.; Califano, V. *Macromolecules* **2003**, *36*, 685.
(37) Guerra, G.; Manfredi, C.; Rapacciuolo, M.; Corradini, P.; Mensitieri, G.; Del Nobile, M. A. Italian Patent, 1994 (C.N.R.).
(38) Manfredi, C.; Del Nobile, M. A.; Mensitieri, G.; Guerra, G.; Rapacciuolo M. *J. Polym. Sci., Polym. Phys. Ed.* **1997**, *35*, 133.
(39) Reverchon, E.; Guerra, G.; Venditto, V. *J. Appl. Polym. Sci.* **1999**, *74*, 2077.
(40) Guerra, G.; Milano, G.; Venditto, V.; Musto, P.; De Rosa, C.; Cavallo, L. *Chem. Mater.* **2000**, *12*, 363.
(41) Milano, G.; Venditto, V.; Guerra, G.; Cavallo, L.; Ciambelli, P.; Sannino, D. *Chem. Mater.* **2001**, *13*, 1506.
(42) Mensitieri, G.; Venditto, V.; Guerra, G. *Sens. Actuators, B* **2003**, *92*, 255.
(43) Guerra, G.; Dal Poggetto, F.; Iuliano, M.; Manfredi, C. *Makromol. Chem.* **1992**, *193*, 2413.
(44) (a) Palin, D. E.; Powell, H. M. *J. Chem. Soc.* **1947**, 208. (b) Tse, J. S.; Ripmeester, J. A. *J. Phys. Chem.* **1983**, *87*, 1708.

MA034678L